

# MEDEA: MULTI-VIEW EFFICIENT DEPTH ADJUSTMENT

Mikhail Artemyev, Anna Vorontsova, Anna Sokolova, and Alexander Limonov

Samsung Research

## ABSTRACT

The majority of modern single-view depth estimation methods predict relative depth and thus cannot be directly applied in many real-world scenarios, despite impressive performance in the benchmarks. Moreover, single-view approaches cannot guarantee consistency across a sequence of frames. Consistency is typically addressed with test-time optimization of discrepancy across views; however, it takes hours to process a single scene. In this paper, we present MEDeA, an efficient multi-view test-time depth adjustment method, that is an order of magnitude faster than existing test-time approaches. Given RGB frames with camera parameters, MEDeA predicts initial depth maps, adjusts them by optimizing local scaling coefficients, and outputs temporally-consistent depth maps. Contrary to test-time methods requiring normals, optical flow, or semantics estimation, MEDeA produces high-quality predictions with a depth estimation network solely. Our method sets a new state-of-the-art on TUM RGB-D, 7Scenes, and ScanNet benchmarks and successfully handles smartphone-captured data from ARKitScenes dataset.

**Index Terms**— consistent depth estimation, test-time optimization

## 1. INTRODUCTION

Depth estimation is a core technology for image and video processing, serving many downstream tasks, such as 3D scene reconstruction, video stabilization, applying a bokeh effect, etc. Compared to other geometric representations, such as voxels, point clouds, implicit neural representations, or truncated signed distance functions (TSDF), representation in a form of 2D depth maps is memory-efficient and suitable for real-time processing.

Existing single-view depth estimation models predict depth either up-to-shift-and-scale, up-to-scale, or in absolute values (metric).

Both up-to-shift-and-scale [5] and up-to-scale [6] methods are inconsistent by design: the depth scale may fluctuate significantly throughout a video sequence, so predicted depth maps do not align in 3D space. Metric depth estimation methods provide scale-aligned outputs across a set of frames, yet processing frames individually inevitably leads to inconsistent predictions. Accordingly, single-view depth predictions

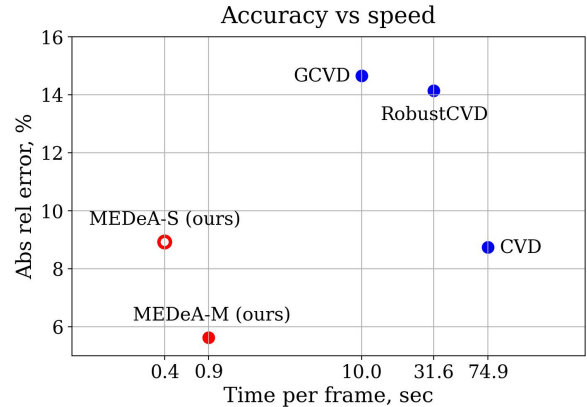


**Fig. 1:** Comparison of depth estimation errors and runtime on the TUM-RGBD dataset [1]. The proposed MEDeA surpasses existing test-time optimization methods (CVD [2], RobustCVD [3], and GCVD [4]) in both accuracy and speed. Our flagship MEDeA-M model outperforms competitors by a huge margin, and even our fast MEDeA-S delivers higher quality than existing approaches with a 25x speed up. Seconds per frame are in logarithmic scale for visibility.

require additional alignment if aiming at video depth estimation.

Several video depth estimation methods actually follow this paradigm, performing test-time optimization of depth priors obtained with a single-view model [2, 3, 4]. Currently, inference speed is the main limitation of test-time optimization methods, making real-time performance unattainable. We are the first to propose the test-time depth optimization method that is on par with feed-forward approaches in speed.

Another way to use information from several frames is a multi-view stereo (MVS) paradigm. Given camera parameters, MVS approaches [7, 8, 9, 10, 11] estimate metric depth. However, since they do not minimize between-frame discrepancy directly, thus cannot guarantee temporal consistency.

Our main contributions are as follows:

- We introduce MEDeA for **fast test-time video depth estimation**, which is on par with feed-forward models in speed, and is an order of magnitude faster than competing test-time optimization approaches;
- We show that consistent video depth estimation can be

addressed with a **minimal pipeline without any auxiliary modules** for optical flow estimation, surface normal estimation, or segmentation;

- With our **novel depth scale propagation strategy**, which enforces the multi-frame coherence and speeds up the convergence, MEDeA sets a new state-of-the-art in video depth estimation. It outperforms existing single-view, MVS, and test-time depth estimation methods in the TUM RGB-D, 7Scenes, and ScanNet benchmarks, while the experiments on the ARK-itScenes show that MEDeA can handle smartphone data available in mobile applications.

## 2. RELATED WORK

We overview existing depth estimation methods that are applicable for videos: single-view, multi-view, and test-time optimization approaches.

### 2.1. Single-view Depth Estimation

To handle a variety of real scenes, a single-view depth estimation should generalize over diverse domains. MiDaS [5] is a seminal work on general-purpose depth estimation, that proposes a scheme of training on a mixture of datasets to generalize over real data, however, it predicts depth up to an unknown shift and scale. Romanov et al. [6] improves MiDaS training scheme to achieve up-to-scale depth estimation with a lightweight model. Recent ZoeDepth [12] fine-tunes MiDaS for metric depth estimation, but still experience generalization issues, similar to other approaches that predict absolute depth. Besides, ZoeDepth relies on a large backbone, resulting in a slow inference comparable to some MVS methods.

### 2.2. Multi-view Depth Estimation

MVS methods improve over single-view approaches by aggregating information from several frames. Most learning-based MVS methods apply plane-sweeping to generate a cost volume. MVSNet [9] and DPSNet [13] build 4D feature volumes and process them with computationally-demanding 3D convolutions, while MVDepthNet [14] directly generates 3D volumes by calculating cost on images by 2D convolutions. DELTAS [15] learns to detect and triangulate keypoints, and converts the sparse set of 3D points into dense depth maps.

Some learning-based MVS approaches also exploit spatial similarity of consequent frames: e.g., GP-MVS [16] extends MVDepthNet [14] with Gaussian Process conditioned on a similarity between camera poses, and DeepVideoMVS [11] training a spatio-temporal Conv-LSTM network for early-stage cost volume fusion. SimpleRecon [7] processes a plane-sweep feature volume without costly 3D convolutions, achieving high efficiency.

When estimating depth for a target frame, MVS methods do not take other depth predictions into account. This results in a low between-frame correlation of depth errors, so there is room for consistency improvement.

### 2.3. Test-time Depth Optimization

CVD [2] is a pioneer approach improving between-frame consistency through test-time optimization. CVD leverages COLMAP camera poses, and fine-tunes a pre-trained depth estimation model using reprojection-based losses. RobustCVD [3] freezes a pre-trained depth estimation model and jointly estimates poses and depth scale maps. GCVD [4] speeds up the scale maps estimation, and ensures global consistency for long videos by integrating a keyframe-based pose graph into learning. IronDepth [17] exploits a pre-trained normal estimation network and uses predicted surface normals to guide the recurrent refinement of depth maps.

All these test-time optimization methods apply auxiliary models for optical flow estimation and dynamic objects segmentation [2, 3, 4], or surface normals estimation [17]. In contrast, we only use a pre-trained single-view depth estimation network. Unlike CVD [2] and GCVD [4], we keep it frozen to avoid costly gradient backpropagation through the model. Furthermore, we propose using the depth estimation network as a feature extractor, and additionally guide the optimization via a feature-metric loss inspired by [18].

RobustCVD [3] and GCVD [4] use MiDaS [5] to obtain initial depth. Yet, they adjust only the scale – while MiDaS actually predicts inverse depth up-to-shift-and-scale, so an inverse depth shift in predictions remains uncompensated. Surprisingly, this issue has been neither empirically investigated nor discussed. In MEDeA, we use a lightweight up-to-scale model by Romanov et al. [6] for initial depth estimation, which requires 12.9x less FLOPs than MiDaS.

## 3. PROPOSED METHOD

For the  $i$ -th frame, we use a pre-trained and frozen depth estimation network to estimate a depth map  $D_i^0$  and extract image features  $F_i$  (so that feature extraction does not require any additional computation). Then, we adjust  $D_i^0$ , resulting in temporally-consistent depth maps  $D_i$  (Fig. 2).

### 3.1. Depth Estimation Network

We leverage the efficient single-view backbone EfficientNet-b5-LRN from Romanov et al. [6] in MEDeA-S, and the accurate multi-view SimpleRecon [7] in MEDeA-M. The experiments show that MEDeA is compatible with such distinct models, and robustly improves their performance in the standard tests. Since MEDeA does not impose any specific limitations, we assume that any single- or multi-view method can be incorporated into our pipeline.

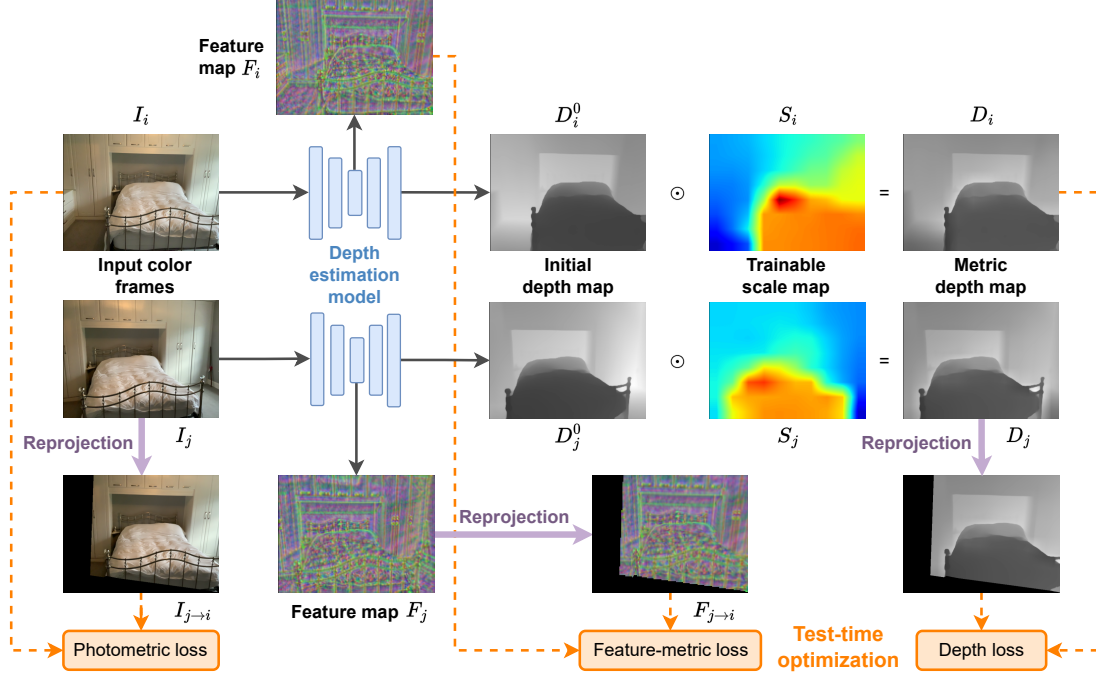


**Fig. 2:** Overview of MEDeA. MEDeA relies on a depth estimation model that outputs either metric or up-to-scale depth maps  $D^0$ . In our depth deformation model, a depth map  $D$  is estimated as an initial depth map  $D^0$  multiplied by a depth scale map  $S$ :  $D = D^0 \odot S$ . At each iteration, a pair of RGB-D frames with indices  $(i, j)$  is selected, and  $S_i, S_j$  are adjusted. Using the current estimate of  $D_i$ , MEDeA reprojects an image  $I_j$ , a depth map  $D_j$ , and a feature map  $F_j$  onto the  $i$ -th viewpoint, and penalizes the divergence of the reprojected  $\{I_{j \rightarrow i}, D_{j \rightarrow i}, F_{j \rightarrow i}\}$  and the original  $\{I_i, D_i, F_i\}$  values. Depth scale maps  $S_i, S_j$  are optimized via backpropagation. As a result, MEDeA provides consistent depth maps  $D_i, D_j$ .

### 3.2. Depth Deformation Model

For a frame  $F_i$ , a *depth scale map*  $S_i$  is estimated in test-time optimization, and the final depth prediction is calculated as:

$$D_i = D_i^0 \odot S_i. \quad (1)$$

Same as RobustCVD [3] and GCVD [4], we use a parametric depth deformation model to adjust depth predictions; we keep the same simple spatially-varying depth scale model to control the computational complexity. In such a model,  $S_i$  is a bilinear spline:

$$S_i = B(\exp(l_i), H, W), \quad (2)$$

where  $l_i$  is a trainable tensor of size of  $h \times w$ , and  $B(*, H, W)$  denotes the bilinear interpolation into the frame resolution  $H \times W$ . Hence, local scale coefficients are defined on a regular grid: for each pixel in a grid cell, the four values in the cell vertices are bilinearly interpolated to get a scaling factor.

### 3.3. Test-time Optimization

Our optimization relies on a reprojection induced by the depth for the  $i$ -th frame. Specifically, we reproject an image  $I_j$ , image features  $F_j$ , and a scale-adjusted depth map  $D_j$  w.r.t the

pose of  $i$ -th frame, using camera poses and intrinsic parameters, to get a pseudo image  $I_{j \rightarrow i}$ , pseudo feature map  $F_{j \rightarrow i}$ , and a pseudo depth map  $D_{j \rightarrow i}$ , respectively. Ideally, the pseudo color, depth map, and feature map should coincide with the original ones, so we penalize their divergence.

The optimization runs in two stages: at the Stage I, depth scale maps are optimized for keyframes only. Then, the depth scale is propagated from keyframes to other frames. At the Stage II, all frames are involved in optimization.

### 3.4. Sampling Frame Pairs

Following CVD [2], we use a hierarchical sampling scheme. Let us denote

$$\text{Pairs}(a, b) = \left\{ (i, j) \mid |i - j| = 2^l, i \bmod 2^l = 0, a \leq l \leq b \right\} \quad (3)$$

Unlike CVD, we sample two sets of frame pairs:  $P_I = \text{Pairs}(3, 6)$  (keyframes,  $K = \bigcup P_I$ ), and  $P_{II} = \text{Pairs}(0, 2)$ .

During the Stage I, we select keyframe pairs  $(i, j)$  uniformly from  $P_I$ . During the Stage II, we update depth scale maps  $l_i$  for  $i \notin K$ . We freeze parameters  $\{l_i \mid i \in K\}$  and optimize w.r.t. frame pairs from  $P_{II}$  solely.

### 3.5. Depth Scale Propagation

As a result of the Stage I, we obtain consistent depth maps for keyframes  $K$ . They are a valuable source of depth scale information, which can be propagated to non-keyframes. Therefore, the optimization at the Stage II can start from a reasonable scale approximation.

For a target non-keyframe with an index  $i \notin K$ , we select the temporally-nearest keyframe with an index  $j \in K$ , and analytically derive  $l_i$  that minimizes  $\mathcal{L}_{\text{depth}}(i, j)$  (see Subsec. 3.6). By dividing the reprojected depth  $D_{j \rightarrow i}$  by an initial depth map  $D_i^0$ , we obtain a depth scale map  $\hat{S}_i = D_{j \rightarrow i} / D_i^0$ . Finally, we calculate the initial parameters of the depth deformation model for the  $i$ -th frame as:

$$l_i := \log(\text{Pool}(\hat{S}_i, h, w)), \quad (4)$$

where  $\text{Pool}(*, h, w)$  denotes pooling into size  $(h, w)$ . We use median pooling to ensure the robustness of scale estimation.

### 3.6. Losses

First, the *photometric loss*  $\mathcal{L}_{\text{photo}}$  forces a pseudo color  $I_{j \rightarrow i}(p)$  of a pixel  $p$  to be consistent with a color  $I_i(p)$ :

$$\mathcal{L}_{\text{photo}}(i, j) = \frac{1}{3|I_{j \rightarrow i}|} \sum_{p \in I_{j \rightarrow i}} \sum_{c=1}^3 |I_i(p, c) - I_{j \rightarrow i}(p, c)|, \quad (5)$$

where  $|I_{j \rightarrow i}|$  is a number of valid pixels in a pseudo image  $I_{j \rightarrow i}$ . Following GCVD [4], we use a *depth loss*  $\mathcal{L}_{\text{depth}}$  bringing a pseudo depth  $D_{j \rightarrow i}(p)$  of a pixel  $p$  closer to  $D_i(p)$ :

$$\mathcal{L}_{\text{depth}}(i, j) = \frac{1}{|I_{j \rightarrow i}|} \sum_{p \in I_{j \rightarrow i}} |D_i(p) - D_{j \rightarrow i}(p)| \quad (6)$$

The *feature-metric*  $\mathcal{L}_{\text{feat}}$  ensures that  $F_{j \rightarrow i}$  and  $F_i$  are alike. For MEDeA-S, we formulate the feature distance as:

$$\mathcal{L}_{\text{feat}}(i, j) = \frac{1}{C|I_{j \rightarrow i}|} \sum_{p \in I_{j \rightarrow i}} \sum_{c=1}^C \frac{|F_i(p, c) - F_{j \rightarrow i}(p, c)|}{|F_i(p, c) + F_{j \rightarrow i}(p, c)|}, \quad (7)$$

SimpleRecon [7] calculates cost volume using dot product of  $F_i$ . Accordingly, we define our feature-metric loss for MEDeA-M as the negative average dot product of  $F_i$  and  $F_{j \rightarrow i}$ :

$$\mathcal{L}_{\text{feat}}(i, j) = -\frac{1}{|I_{j \rightarrow i}|} \sum_{p \in I_{j \rightarrow i}} F_i(p) \cdot F_{j \rightarrow i}(p) \quad (8)$$

The total loss  $\mathcal{L}(i, j)$  is a sum of losses  $\mathcal{L}(i, j) = \mathcal{L}_{\text{photo}}(i, j) + \mathcal{L}_{\text{depth}}(i, j) + \mathcal{L}_{\text{feat}}(i, j)$ .

## 4. EXPERIMENTS

### 4.1. Datasets

We evaluated our method on TUM RGB-D [19], 7Scenes [20], and ScanNet [21] indoor benchmarks, following the evaluation protocol of DeepVideoMVS [11]. Moreover, we included ARKitScenes [1] as an in-the-wild benchmark. This

large-scale dataset, collected using a tablet with an online ARKit tracking system, features noisy camera poses and fast camera movements. We evaluate on the first 25 sequences longer than 20 seconds from the validation subset, for which the corresponding RGB and ground truth depth are available.

### 4.2. Evaluation Protocol

We evaluate our approach in two set-ups. First, we focus on depth estimation solely, assuming that ground truth camera poses are available. Alternatively, we emulate usage without given camera poses and estimate up-to-scale camera poses with DROID-SLAM [22]. The quality is measured with the standard metrics [5, 6, 12]: *abs rel*, *abs diff* and  $\delta < 1.25$ .

### 4.3. Implementation Details

All experiments are performed on a single Tesla P40 GPU.

In MEDeA-S, we extract features  $F$  from the encoder block 3 of the backbone (chosen empirically). In MEDeA-M, we use the output of SimpleRecon [7] feature encoder, as these features were trained to match across different frames.

Images are resized with a scale of 1/4. The size of log-scale tensors  $l_i$  is (8, 10) for horizontal and (10, 8) for vertical videos. Before adjustment,  $l_i$  are initialized with  $\log(1) = 0$ . Then, they are updated using Adam optimizer with a batch size of 128 frame pairs. The learning rate is set to 0.1 and degrades exponentially with  $\gamma = 0.996$  at Stage I and  $\gamma = 0.96$  at Stage II. Stage I and Stage II last for 600 and 60 epochs. The optimization stops when the loss does not reduce by at least 1% throughout 40 epochs at the Stage I and 4 epochs at the Stage II.

## 5. RESULTS

### 5.1. Comparison to Prior Work

#### 5.1.1. Competitors

We evaluate MEDeA against various depth estimation approaches. ZoeDepth [12] (metric) and Romanov et al. [6] (up-to-scale) represent the single-view paradigm. Then, we report results of MVS approaches [11, 13, 14, 15, 16], including SimpleRecon [7].

We also compare against test-time optimization approaches. CVD [2] uses COLMAP poses and predicts up-to-scale depth. RobustCVD [3] and GCVD [4] estimate camera poses and depth maps jointly, hence providing up-to-scale predictions. Surprisingly, these methods do not benefit from using ground truth poses: we attribute this to the joint training procedure, causing depth estimation errors to be partially compensated with camera pose drifts.

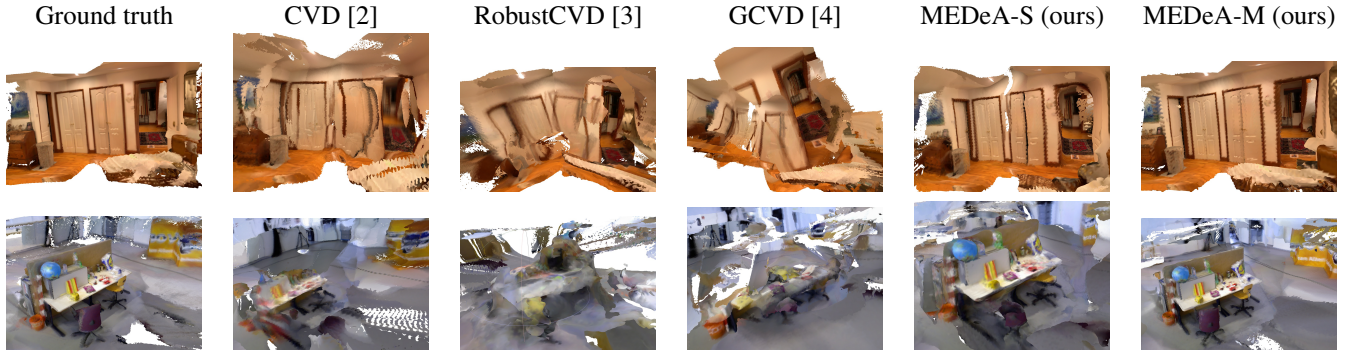


**Fig. 3:** ARKitScenes (top) and TUM RGB-D (bottom) scenes, reconstructed using depth maps produced by different test-time optimization methods, including MEDeA. For a fair comparison, we do not use ground truth camera poses but estimate them with DROID-SLAM [22]. Obviously, other methods struggle to restore a general scene structure, while MEDeA provides well-aligned scans with fewer visual artifacts.

**Table 1:** Results of metric depth estimation methods. No additional scale alignment is applied prior to this evaluation. The best scores are **bold**, the second best are underlined.

Method		TUM RGB-D			7Scenes			ScanNet			ARKitScenes		
		abs diff [m]↓	abs rel [%]↓	$\delta_{1.25}$ [%]↑	abs diff [m]↓	abs rel [%]↓	$\delta_{1.25}$ [%]↑	abs diff [m]↓	abs rel [%]↓	$\delta_{1.25}$ [%]↑	abs diff [m]↓	abs rel [%]↓	$\delta_{1.25}$ [%]↑
Single-view	ZoeDepth [12]	0.461	20.6	65.7	0.349	23.2	66.5	0.600	53.0	31.7	0.286	19.5	75.0
Multi-view	MVDepthNet [14]	0.290	11.7	86.0	0.203	11.6	86.9	0.165	8.5	92.8	-	-	-
	DPSNet [13]	0.326	13.4	83.1	0.249	14.8	82.6	0.155	8.0	93.3	-	-	-
	DELTA [15]	0.353	12.7	81.8	0.191	11.4	88.2	0.150	7.9	93.8	-	-	-
	GP-MVS [16]	<u>0.244</u>	10.4	88.9	0.196	11.8	87.2	0.149	7.6	94.0	-	-	-
	DeepVideoMVS [11]	0.288	9.8	88.5	0.145	8.3	93.8	0.119	5.8	96.7	-	-	-
	SimpleRecon [7]	0.262	<u>7.9</u>	<u>89.6</u>	<u>0.105</u>	<u>5.8</u>	<b>97.4</b>	<b>0.087</b>	<u>4.3</u>	<u>98.1</u>	<u>0.117</u>	<u>7.8</u>	<u>93.2</u>
Test-time optim.	MEDeA-S (ours)	0.515	17.0	73.0	0.158	8.3	91.0	0.193	9.5	89.5	0.182	12.2	84.5
	<b>MEDeA-M (ours)</b>	<b>0.208</b>	<b>6.4</b>	<b>93.0</b>	<b>0.094</b>	<b>5.0</b>	<u>97.0</u>	<u>0.088</u>	<b>4.2</b>	<b>98.2</b>	<b>0.108</b>	<b>7.1</b>	<b>93.6</b>

**Table 2:** Results of up-to-scale depth estimation methods, that do not have access to ground truth poses. MEDeA relies on camera poses from DROID-SLAM [22]. Predicted depth maps are scale-aligned with ground truth ones prior to the evaluation.

Method		TUM RGB-D			7Scenes			ARKitScenes		
		abs diff [m]↓	abs rel [%]↓	$\delta_{1.25}$ [%]↑	abs diff [m]↓	abs rel [%]↓	$\delta_{1.25}$ [%]↑	abs diff [m]↓	abs rel [%]↓	$\delta_{1.25}$ [%]↑
Single-view	Romanov et al. [6]	0.320	14.3	82.2	0.216	12.3	83.7	0.230	15.7	78.6
Test-time optim.	RobustCVD [3]	0.452	19.3	66.8	0.403	21.7	56.8	0.387	23.8	63.9
	GCVD [4]	0.643	29.6	51.0	0.391	21.1	57.0	0.587	45.3	41.8
	MEDeA-S (ours)	<u>0.221</u>	<u>9.2</u>	<u>89.2</u>	<u>0.137</u>	<u>7.4</u>	<u>92.5</u>	<u>0.150</u>	<u>9.9</u>	<u>88.3</u>
	<b>MEDeA-M (ours)</b>	<b>0.139</b>	<b>5.5</b>	<b>95.5</b>	<b>0.066</b>	<b>3.5</b>	<b>97.6</b>	<b>0.096</b>	<b>6.1</b>	<b>93.7</b>

### 5.1.2. Quantitative Results

Tab. 1 proves test-time optimization to improve over state-of-the-art MVS approaches. Evidently, MVS strategies of ag-

gregating spatial information are suboptimal, and there is still room for enhancement. Since consistency is a prerequisite for accuracy, addressing inconsistency with a direct optimization improves individual depth maps. The gain w.r.t the single-

**Table 3:** Comparison with CVD [2] on TUM RGB-D sequences where COLMAP succeeded. MEDeA uses camera poses from DROID-SLAM [22]. Predicted depth maps are scale-aligned with ground truth ones prior to the evaluation.

Method	abs diff [m]↓	abs rel [%]↓	$\delta_{1.25}$ [%]↑	Time per frame [sec]↓
CVD [2]	0.200	8.7	90.5	74.9
RobustCVD [3]	0.312	14.1	82.5	31.6
GCVD [4]	0.315	14.7	80.4	10.0
MEDeA-S (ours)	0.215	8.9	89.5	<b>0.44</b>
<b>MEDeA-M (ours)</b>	<b>0.128</b>	<b>5.6</b>	<b>94.9</b>	<u>0.88</u>

view metric ZoeDepth [12] method is even more tangible, especially on 7Scenes and ScanNet. SimpleRecon [7] is trained on ScanNet, so the gain is more prominent on other datasets, proving better generalization of MEDeA.

In Tab. 2, we compare test-time optimization approaches. As they predict depth up to scale, we align the depth maps with ground truth ones before computing metrics. We omit ScanNet here, since the test-time optimization would take up to six GPU-months for competing approaches [2, 3, 4]. Evidently, MEDeA outperforms others by a large margin, and sets a new strong state-of-the-art in video depth estimation. Besides, MEDeA-S demonstrates a solid gain over initial single-view predictions by Romanov et al. [6], proving the viability of our approach.

We also evaluate against the seminal test-time optimization CVD [2] on TUM RGB-D. CVD [2] estimates camera poses with COLMAP, which succeeds on 8 out of 13 test videos [11], so we compare other test-time optimization methods on the same videos. As shown in Tab. 3, apart from superior depth estimation quality, MEDeA is significantly faster than the competing approaches.

### 5.1.3. Qualitative Results

Consistent depth maps allow obtaining precise 3D scans, while any severe inconsistencies would reveal themselves clearly as reconstruction artifacts. To demonstrate the superior consistency of depth maps produced by MEDeA in comparison with other consistent depth estimation methods, we use these maps to reconstruct scenes via TSDF fusion, and visualize the scans in Fig. 3. As one can see from a side-by-side comparison, our depth adjustment approach provides well-aligned reconstructions with a clear scene structure.

## 5.2. Ablation Study

To provide a comprehensive study of MEDeA, we run additional experiments focusing on different aspects. In the ablation study, we use TUM RGB-D, since this benchmark is arguably the most commonly used and hence well-studied.

**Table 4:** Ablation study of losses on TUM RGB-D.

Method	abs diff [m]↓	abs rel [%]↓	$\delta_{1.25}$ [%]↑	Time per frame [sec]
MEDeA-M	<b>0.208</b>	<b>6.4</b>	<b>93.0</b>	0.88
w/o $\mathcal{L}_{\text{photo}}$	<u>0.213</u>	<u>6.5</u>	<u>92.8</u>	0.86
w/o $\mathcal{L}_{\text{depth}}$	0.386	15.2	77.5	0.85
w/o $\mathcal{L}_{\text{feat}}$	0.285	9.1	88.7	0.85

**Table 5:** Effect of depth scale propagation on TUM RGB-D.

Method	abs diff [m]↓	abs rel [%]↓	$\delta_{1.25}$ [%]↑
MEDeA-M	<b>0.208</b>	<b>6.4</b>	<b>93.0</b>
w/o scale propagation	0.284	9.1	88.7

### 5.2.1. Losses

We run MEDeA with different loss terms. According to the Tab. 4, both depth and feature-metric losses have a major impact on the accuracy. The photometric loss does not add much to the performance: it might be redundant when feature-metric loss is applied, as features already contain sufficient information about objects’ appearance. Using all losses ensures the best results, while the computational overhead is minor.

### 5.2.2. Depth Scale Propagation

To prove our depth scale propagation, we try initializing the non-keyframe depth scale maps with ones, same as for keyframes at the Stage I. Evidently, turning our novel depth scale propagation scheme off worsens all the scores, while the improvement of inference speed is negligible (Tab. 5). So, we can confidently conclude that depth estimation benefits from initializing depth scale maps by reprojection.

## 6. CONCLUSION

We presented MEDeA, that addresses depth estimation from videos. MEDeA obtains depth priors with a pre-trained network, and performs inference-time optimization to ensure depth consistency between frames. By using image features to guide the optimization and applying the novel scale propagation strategy, our approach generates high-quality depth maps an order of magnitude faster than the previous state-of-the-art test-time optimization approach. MEDeA outperformed existing single-view, multi-view, and test-time depth estimation approaches on the standard benchmarks and also proved to handle imperfect smartphone-captured data. Overall, we set a new state-of-the-art in video depth estimation in both accuracy and efficacy.

## 7. REFERENCES

- [1] Gilad Baruch, Zhuoyuan Chen, Afshin Dehghan, Tal Dimry, Yuri Feigin, Peter Fu, Thomas Gebauer, Brandon Joffe, Daniel Kurz, Arik Schwartz, and Elad Shulman, "ARKitScenes - a diverse real-world dataset for 3d indoor scene understanding using mobile RGB-d data," in *Neural Information Processing Systems (NeurIPS) Datasets and Benchmarks Track*, 2021.
- [2] Xuan Luo, Jia-Bin Huang, Richard Szeliski, Kevin Matzen, and Johannes Kopf, "Consistent video depth estimation," vol. 39, no. 4, 2020.
- [3] Johannes Kopf, Xuejian Rong, and Jia-Bin Huang, "Robust consistent video depth estimation," in *Computer Vision and Pattern Recognition (CVPR)*, 2021.
- [4] Yao-Chih Lee, Kuan-Wei Tseng, Guan-Sheng Chen, and Chu-Song Chen, "Globally consistent video depth and pose estimation with efficient test-time training," *arXiv*, 2022.
- [5] René Ranftl, Katrin Lasinger, David Hafner, Konrad Schindler, and Vladlen Koltun, "Towards robust monocular depth estimation: Mixing datasets for zero-shot cross-dataset transfer," *Transactions on Pattern Analysis and Machine Intelligence (TPAMI)*, 08 2020.
- [6] Mikhail Romanov, Nikolay Patatkin, Anna Vorontsova, Sergey Nikolenko, Anton Konushin, and Dmitry Senyushkin, "Towards general purpose geometry-preserving single-view depth estimation," *arXiv*, 2021.
- [7] Mohamed Sayed, John Gibson, Jamie Watson, Victor Prisacariu, Michael Firman, and Clément Godard, "Simplerecon: 3d reconstruction without 3d convolutions," in *European Conference on Computer Vision (ECCV)*, 2022.
- [8] Po-Han Huang, Kevin Matzen, Johannes Kopf, Narendra Ahuja, and Jia-Bin Huang, "Deepmvs: Learning multi-view stereopsis," in *Computer Vision and Pattern Recognition (CVPR)*, 2018.
- [9] Yao Yao, Zixin Luo, Shiwei Li, Tian Fang, and Long Quan, "Mvsnet: Depth inference for unstructured multi-view stereo," in *European Conference on Computer Vision (ECCV)*, 2018.
- [10] Xiaoxiao Long, Lingjie Liu, Wei Li, Christian Theobalt, and Wenping Wang, "Multi-view depth estimation using epipolar spatio-temporal networks," in *Computer Vision and Pattern Recognition (CVPR)*, 06 2021, pp. 8258–8267.
- [11] Arda Duzceker, Silvano Galliani, Christoph Vogel, Pablo Speciale, Mihai Dusmanu, and Marc Pollefeys, "Deepvideomvs: Multi-view stereo on video with recurrent spatio-temporal fusion," in *Computer Vision and Pattern Recognition (CVPR)*, 2021.
- [12] Shariq Farooq Bhat, Reiner Birkel, Diana Wofk, Peter Wonka, and Matthias Müller, "Zoedepth: Zero-shot transfer by combining relative and metric depth," *arXiv*, 2023.
- [13] Sunghoon Im, Hae-Gon Jeon, Stephen Lin, and In-So Kweon, "Dpsnet: End-to-end deep plane sweep stereo," *arXiv*, vol. abs/1905.00538, 2019.
- [14] Kaixuan Wang and Shaojie Shen, "Mvdepthnet: real-time multiview depth estimation neural network," in *International Conference on 3D Vision (3DV)*, 2018.
- [15] Ayan Sinha, Zak Murez, James Bartolozzi, Vijay Badrinarayanan, and Andrew Rabinovich, "Deltas: Depth estimation by learning triangulation and densification of sparse points," in *European Conference on Computer Vision (ECCV)*, 2020.
- [16] Yuxin Hou, Juho Kannala, and A. Solin, "Multi-view stereo by temporal nonparametric fusion," in *International Conference on Computer Vision (ICCV)*, 2019.
- [17] Gwangbin Bae, Ignas Budvytis, and Roberto Cipolla, "Irondepth: Iterative refinement of single-view depth using surface normal and its uncertainty," in *British Machine Vision Conference (BMVC)*, 2022.
- [18] Chang Shu, Kun Yu, Zhixiang Duan, and Kuiyuan Yang, "Feature-metric loss for self-supervised learning of depth and egomotion," in *European Conference on Computer Vision (ECCV)*, 2020.
- [19] J. Sturm, N. Engelhard, F. Endres, W. Burgard, and D. Cremers, "A benchmark for the evaluation of rgb-d slam systems," in *International Conference on Intelligent Robot Systems (IROS)*, 10 2012.
- [20] Jamie Shotton, Ben Glocker, Christopher Zach, Shahram Izadi, Antonio Criminisi, and Andrew Fitzgibbon, "Scene coordinate regression forests for camera relocalization in rgb-d images," in *Conference on Computer Vision and Pattern Recognition (CVPR)*, 06 2013.
- [21] Angela Dai, Angel X. Chang, Manolis Savva, Maciej Halber, Thomas Funkhouser, and Matthias Nießner, "ScanNet: Richly-annotated 3d reconstructions of indoor scenes," in *Computer Vision and Pattern Recognition (CVPR)*, 2017.
- [22] Zachary Teed and Jia Deng, "Droid-slam: Deep visual slam for monocular, stereo, and rgb-d cameras," in *Neural Information Processing Systems (NeurIPS)*, 2021.